

# Experimental study of the feasibility of phosphorus-32 as a new energy source to treat difficult tachycardia originating from around the coronary artery

**Qingyong Chen**

West China Hospital of Sichuan University

**Wen Yue**

West China Hospital of Sichuan University

**Tengda Chen**

West China Hospital of Sichuan University

**Bosen Yang**

West China Hospital of Sichuan University

**Qing Yang** (✉ [qingyang@scu.edu.cn](mailto:qingyang@scu.edu.cn))

West China Hospital of Sichuan University

---

## Article

**Keywords:** ventricular arrhythmias, internal radiotherapy, phosphorus-32

**Posted Date:** May 25th, 2022

**DOI:** <https://doi.org/10.21203/rs.3.rs-1612814/v1>

**License:**   This work is licensed under a Creative Commons Attribution 4.0 International License.

[Read Full License](#)

---

# Abstract

Tachyarrhythmia originating from around the coronary artery remains a great clinical challenge for electrophysiologists. This study explored the feasibility of using phosphorus-32 (P-32) as a new energy source to treat tachyarrhythmia around the coronary artery. Four points of the left ventricle of seven Bama mini-pigs and femoral artery of pig4-7 were selectively radiated in protocol by a self-designed radiation catheter. The voltage mapping showed a significantly lower voltage at the irradiated sites 30 days after the procedure compared with that before the irradiation for pigs2-7 1.77 vs 4.39 p 0.001 . No obvious stenosis was observed in the coronary artery and femoral artery at the irradiation site. P-32 internal radiotherapy can change the electrical properties of cardiomyocytes, but it has few effects on the coronary and femoral artery. P-32 could be a complementary or alternative treatment for tachyarrhythmia originating from around the coronary artery.

## Introduction

The aim of radiofrequency catheter ablation (RFCA) for the treatment of tachyarrhythmia is to destroy cardiomyocytes at the origin or key isthmus by causing them to experience coagulative necrosis so that they no longer emit impulses or form reentrant pathways[1]. Our previous studies have shown that the main reason for tachyarrhythmia refractory to RFCA is that the complicated local anatomy and the origins of the arrhythmia (or key isthmus) are not only myocardial tissues but also important vascular tissues, such as coronary arteries. Although ablation of these origin sites can cause cardiomyocyte necrosis of the lesion, it may also damage blood vessels, thus leading to extremely serious complications, such as acute myocardial infarction or vascular rupture. Therefore, tachyarrhythmia originating from around the coronary artery remains a great clinical challenge for electrophysiologists. None of the currently available ablation energy sources, including the most commonly used radiofrequency current energy sources, such as direct current, lasers, microwaves, ultrasound, freezing energy, and pulsed electric fields[2-4], which have recently been used in clinical practice, can solve this problem. It can be inferred that if an energy source can be found that can destroy myocardial tissues and cause cardiomyocyte necrosis but has little or no effect on the blood vessels, the treatment of difficult tachyarrhythmia can become a possibility. Moreover, because the areas of origin of the arrhythmia or key isthmus are usually small (most are several mm<sup>2</sup>), it is usually necessary to accurately locate the area to determine its exact location. Three-dimensional mapping involving electric or magnetic fields, which is widely used in clinical practice[5], is designed for this purpose. The energy source must accurately reach these positions; therefore, its volume must be miniaturized so that it can be simultaneously integrated with the mapping electrode. A three-dimensional mapping system involving the electric or magnetic field can identify the mapping electrode, which combines with the energy source and guides the therapeutic process. Some cases of tachyarrhythmia with failed RFCA have been treated with stereotactic body radiotherapy (SBRT), and short-term benefits have been achieved[6-8]. However, as external radiotherapy, SBRT results in a large irradiation area and can be used only for treating organic ventricular tachycardia, resulting in large scars[9-13]. With idiopathic ventricular tachycardia, which requires precise mapping to determine the

ablation sites, there is a risk of damaging large amounts of normal myocardial tissues because of the major damage caused by SBRT. To overcome the shortcomings of SBRT and combine it with the current RFCA techniques, such as cardiac three-dimensional modeling and voltage mapping, radionuclide-based internal radiotherapy has been used to treat difficult tachyarrhythmia. Radionuclide-based internal radiotherapy may have many advantages, such as small size, easy mapping, and the ability to solve the disadvantages of SBRT (for example, damage to a large area of the myocardium). The radionuclide phosphorus-32 (P-32) is currently used for the treatment of skin keloids and the control of cancerous ascites in certain malignant tumors. Therefore, during this study, P-32 was selected as the experimental radioactive source to observe whether it can effectively damage the myocardium and cause changes in the electrophysiological characteristics of myocardial tissues. Simultaneously, we observed its effects on arteries to determine whether it may be a potential energy source for the treatment of difficult tachyarrhythmia originating from around the coronary artery.

# 1 Experimental Principle And Feasibility

## 1.1 Principle

Radioactive nuclei can spontaneously release particles or rays (such as  $\alpha$ ,  $\beta$ , and  $\gamma$ ) from the unstable nucleus and simultaneously release energy. These rays can interfere with the functions of cellular DNA or RNA, causing cell apoptosis and tissue fiber deposition, thereby changing the electrical activity of cardiomyocytes[14, 15]. To treat difficult tachyarrhythmia originating from around the coronary artery, it is necessary to damage the cardiomyocytes at the origin or conduction pathway of tachyarrhythmia; however, this damage should not affect the coronary artery in cases of myocardial infarction. Compared with normal cardiomyocytes, the cardiomyocytes at the origin of tachyarrhythmia only differ in their electrical activity; there is no difference in their sensitivity to radiation. Therefore, it can be deduced that when radioactive energy can effectively cause damage to normal cardiomyocytes, it can also damage cells at the origin of difficult tachyarrhythmia to achieve arrhythmia treatment.

## 1.2 Feasibility

P-32 is a pure  $\beta$ -decay nuclide. The maximum energy of  $\beta$ -rays is 1.711 MV, and its half-life is 14.3 days. P-32 has been used for the treatment of skin keloids, hemangiomas in children, and cancerous ascites in certain malignant tumors. Its safety and effectiveness are relatively high. Radionuclides can also be used for cardiovascular issues; for example, radioactive stents can be used to treat coronary heart disease. Theoretically, P-32 may also be used to treat arrhythmia.

# 2 Methods

## 2.1 Experimental animals

Seven Bama mini-pigs (pigs 1-7) were provided by Sichuan Greentech Biotechnology Co., Ltd. Their basic characteristics, including weight, age, and sex, are listed in Table 1 (production license number: SYXK

[Sichuan] 2018-212. Pigs were kept in a 12-h light/dark cycle and were free to get food and water. This study was approved by the Biomedical Ethic Committee of West China Hospital of Sichuan University (2020383A), and all of the experiments were performed in accordance with ARRIVE guidelines. Details of the experimental devices and consumables are listed in Table 2. The related experimental drugs are listed in Table 3.

Table 1  
Characteristics of the experimental pigs

Pig	Sex	Weight before the procedure (kg)	Age (month)	Weight at 4 weeks (kg)
1	Female	40	5	44
2	Female	40	5	45
3	Female	50	6	53
4	Male	42	5	44
5	Male	42	5	45
6	Male	40	5	43.5
7	Male	50	6	52

Table 2  
Experimental equipment and consumables

Pig	Products	Manufacturer
1	High-frequency mobile C-arm X-ray machine	Nanjing Puai Medical Equipment Co., Ltd.
2	High-frequency jet ventilator	Jiangxi Teli Anesthesia Respiratory Equipment Co., Ltd.
3	LEAD-mapping cardiac electrophysiology 3D mapping system	Sichuan Jinjiang Electronics Co., Ltd.
4	Body surface reference electrode	Sichuan Jinjiang Electronics Co., Ltd.
5	Magnetically positioning, adjustable, bendable, electrophysiological mapping catheter	Sichuan Jinjiang Electronics Co., Ltd.
6	Magnetically positioning saline perfusion radiofrequency ablation catheter	Sichuan Jinjiang Electronics Co., Ltd.
7	Perfusion pump	Sichuan Jinjiang Electronics Co., Ltd.
8	Multi-conductivity physiological recorder	Sichuan Jinjiang Electronics Co., Ltd.
9	Catheter sheath with hemostatic valve (short sheath)	St. Jude Medical Products Co., Ltd.
10	Catheter sheath with hemostatic valve (long sheath)	St. Jude Medical Products Co., Ltd.
11	Phosphorus-32 source	Atom Technology Co., Ltd.
12	Femoral artery puncture needle	Shanghai Jumu Medical Devices Co., Ltd.

Table 3  
Experimental drugs

Pig	Drug	Manufacturer
1	Zoletil	France Vic Pet Health Company
2	Atropine sulfate injection	Jieyang Animal Pharmaceutical Co., Ltd.
3	Propofol emulsion injection	Guangdong Jiabo Pharmaceutical Co., Ltd.
4	Tramadol hydrochloride injection	Germany Grantai Co., Ltd.
5	Bemiparin sodium injection	Laboratorios Farmacéuti Co., Ltd.
6	Sumianxin II injection	Kunming Pet Pharmaceutical Co., Ltd.

## 2.2 Experimental steps

### 2.2.1 Induced anesthesia

All animals were fasted for 12 h and were not allowed to drink for 4 h before the experiment. At the beginning of the experiment, 5 ml (2.5 mg) of atropine was injected intramuscularly behind the ears. Then, 15 min later, Zoletil (2-5 mg/kg) and Sumianxin II (1.6-4.0 mg/kg) were injected intramuscularly. After being completely anesthetized, the experimental pigs were supported by a ventilator and transported to the catheterization laboratory.

### 2.2.2 Anesthesia maintenance

The experimental pigs were placed on their back in the U-shape groove on the catheter bed. The limbs were fixed with bandages, the tongue was pulled out with sterile forceps, and the upper and lower jaws were isolated with a cork and fixed with bandages. An intravenous channel was established through the ear vein, and propofol injection (approximately 4-12 mg/kg) was administered continuously to maintain anesthesia and sedation. Tramadol hydrochloride injection was continuously administered (approximately 2 mg/kg) for analgesia. The anesthesia dosage was adjusted according to the eyelid, corneal reflex, and limb activity.

### 2.2.3 Procedure steps

#### 2.2.3.1 Femoral artery and vein puncture

After anesthesia, punctures were guided by an ultrasound device and performed from the femoral vein and femoral artery. The femoral vein was implanted with 7-Fr vascular sheaths, and the femoral artery was implanted with 8-Fr vascular sheaths.

### **2.2.3.2 Inserting leads and the catheter**

The ventricular electrode was inserted from the 6-Fr vascular sheath to the apex of the right ventricle, and the coronary sinus electrode was inserted from the 7-Fr vascular sheath to the coronary sinus. The magnetically positioned cold saline perfusion ablation catheter was inserted in the left ventricle through an 8-Fr vascular sheath.

### **2.2.3.3 Modeling and voltage mapping**

The left ventricle electrical anatomical model was created using a magnetically positioned cold saline perfusion ablation catheter. The points to be radiated (one point at the apex, two points at the mitral annulus, and one point at the left coronary sinus) were marked on the electrical anatomical model, and voltage mapping was performed (Fig. 1). Then, the radiofrequency catheter was replaced by a magnetically guided, adjustable, bendable mapping catheter with a P-32 source at the head end.

### **2.2.3.4 Determining the radiation points and doses of internal radiotherapy**

The magnetic positioning function was used to determine the planned points for radiotherapy. The irradiation time for each point in pigs 1 and 2 was 30 min, and that of pig 3 was 60 min. The P-32 source radiation was 13 mCi for those pigs. For pigs 4 to 7, each point received 30 min of P-32 source radiation of 26 mCi. Furthermore, the femoral artery was selectively irradiated for the same time and with the same radiation dose in pigs 4 to 7. The specific exposure doses are shown in Table 4.

### **2.2.3.5 Voltage mapping**

Voltage mapping was performed immediately after internal irradiation, and the changes in the local potential were evaluated. Femoral artery angiography was performed to explore whether arterial stenosis existed 1 month after irradiation.

### **2.2.3.6 Animal sacrifice**

Pig 1 was killed by intravenous injection of 20-30ml of 10% potassium chloride solution on the day of the first procedure. Its heart samples were obtained, fixed, and sliced. Then, a pathological examination was performed. Pigs 2 to 7 were kept alive for 1 month. Then, voltage mapping was conducted again. After that procedure, those pigs were killed by the same method with Pig 1. Cardiac and femoral artery samples were taken from pigs 4 to 7 for pathological examination.

Table 4

Irradiation time, distance, and dose for different points

Pig	Number of irradiated points	Irradiation time (min)	Exposure dose at different distances (Gy)				
			1 mm	2 mm	3 mm	4 mm	5 mm
1	1	30	54	21	7.5	0.9	0.05
	2	30	54	21	7.5	0.9	0.05
	3	30	54	21	7.5	0.9	0.05
	4	30	54	21	7.5	0.9	0.05
2	1	30	54	21	7.5	0.9	0.05
	2	30	54	21	7.5	0.9	0.05
	3	30	54	21	7.5	0.9	0.05
	4	30	54	21	7.5	0.9	0.05
3	1	60	108	42	15	1.8	0.1
	2	60	108	42	15	1.8	0.1
	3	60	108	42	15	1.8	0.1
	4	60	108	42	15	1.8	0.1
4 to 7	1	30	108	42	15	1.8	0.1
	2	30	108	42	15	1.8	0.1
	3	30	108	42	15	1.8	0.1
	4	30	108	42	15	1.8	0.1

### 2.3 Statistical analysis

The parameters are expressed as mean  $\pm$  standard derivation (SD). All data analyses were performed using the SPSS 25 (SPSS, Chicago, IL, USA). Differences were considered significant for all analyses in this study when the probability value was  $<0.05$ . The difference between the two groups was compared by independent sample T-test, and the difference before and after the irradiation was compared by paired sample T-test.

## 3 Results

The procedures were successfully performed for all experimental pigs. No serious complications occurred during the procedure, and no vital signs were obviously unstable after the procedure. For experimental pig

1, there was no significant difference between voltage mapping after the procedure and voltage mapping before the procedure, and the pathological examination results showed no obvious damage. For experimental pigs 2 to 7, the voltage was measured again after 1 month. The voltage of the irradiated points after 1 month was significantly lower than that before irradiation, and the pathological results showed obvious pathological damage.

### **3.1 Comparison of voltage mapping before and immediately after internal radiotherapy**

No significant difference in voltage mapping was observed before or immediately after irradiation in all experimental pigs. This indicates that the damaging effects of P-32 internal radiotherapy require time to become apparent (Fig. 2)..

### **3.2 Comparison of voltage mapping before and 30 days after internal radiotherapy**

The voltage mapping (Figs. 3) showed a significantly lower voltage at the irradiated sites 30 days after the procedure compared with that before the irradiation for pigs 2-7 1.77 vs 4.39 p 0.001 . For pigs 3 to 7, at 30 days after irradiation, voltage mapping also revealed that the potential of the irradiation sites decreased significantly 1.96 vs 4.56 p=0.001 ,with a low-voltage area larger than that of pig 2. The specific decreases are listed in Tables 5 and 6.

Table 5

Voltage changes before and 30 days after internal radiotherapy

Pig	Number of irradiated points	Phosphorus-32 activity (mCi)	Irradiation time (min)	Voltage before the procedure (mV)	Voltage 30 days after the procedure (mV)	Deceased voltage ratio (%)
2	1	13	30	5.64	0.69	87.8
	2	13	30	3.15	0.48	84.8
	3	13	30	3.55	1.48	65.7
	4	13	30	1.84	0.61	66.8
3	1	13	60	3.57	1.19	66.7
	2	13	60	7.94	1.14	85.6
	3	13	60	2.83	0.82	71.0
	4	13	60	1.83	0.40	78.1
4	1	26	30	3.02	1.75	42.1
	2	26	30	7.99	1.69	78.8
	3	26	30	3.02	1.59	47.4
	4	26	30	1.53	0.95	37.9
5	1	26	30	3.39	2.83	16.5
	2	26	30	3.15	1.27	59.7
	3	26	30	6.19	1.16	81.3
	4	26	30	1.51	0.58	61.6
6	1	26	30	7.67	2.59	66.2
	2	26	30	7.94	4.97	37.4
	3	26	30	7.94	4.07	48.7
	4	26	30	2.65	1.22	54.0
7	1	26	30	8.04	4.82	40.0
	2	26	30	7.94	4.82	39.3
	3	26	30	2.43	0.85	65.0
	4	26	30	0.58	0.42	27.6

**Table 6**

## Average voltage changes before and 30 days after internal radiotherapy

Pig	Average voltage before the procedure (mV)	Average voltage 30 days after the procedure (mV)	Mean decreased voltage ratio (%)	P
2	3.55	0.82	76.3	0.016*
3	4.04	0.89	75.4	0.059
4	3.89	1.50	51.6	0.143
5	3.56	1.46	54.8	0.101
6	6.55	3.21	54.00	0.074
7	4.75	2.73	43.0	0.406

\* indicates the difference is significant.

### 3.3 Pathological results immediately after internal radiotherapy

The heart of experimental pig 1 was removed immediately after the procedure, fixed in formalin, and sliced to observe the pathological changes at the four irradiation points. Different degrees of inflammatory cell infiltration were observed using microscopy, including neutrophils, a few eosinophils, lymphocytes, and mononuclear macrophages. Parts of the myocardial tissue showed atrophy and muscle fiber breakage around the irradiated points. Masson staining showed slightly blue-stained fiber tissue accumulations around the interstitium in the myocardium (Fig. 4).

### 3.4 Gross specimen and pathological results 30 days after the procedure

At 30 days after the procedure, the gross specimens showed fibrosis changes of the inner and outer membrane surfaces of the irradiated sites. The pathological results showed obvious fibrosis changes in the irradiated area. The degree of fibrosis was most severe in the area where the radiation dose was the largest Fig.5 .

### 3.5 Effects of phosphorus-32 internal radiotherapy on the femoral artery and coronary artery opening

No obvious stenosis at the irradiated site of the femoral artery or coronary artery (the opening of the right coronary artery) in the gross specimen was observed with the naked eye. Furthermore, no obvious pathological changes of the femoral artery or the opening of the coronary artery were observed with the naked eye. There were no electrocardiogram manifestations of coronary heart disease according to the surface electrocardiogram or intracavitary electrocardiogram before and 30 days after the procedure. Pathological results after the procedure showed that the whole structures of the intima, media, and adventitia were intact; there were only mild inflammatory lesions in the intima of the proximal left anterior descending artery, which was considered to be a reversible injury resulting from the direct contact force of the tip of the catheter (Fig. 6). Femoral arteriography after the procedure showed no significant stenosis

before or 30 days after radiation (Fig. 6). Pathological results showed that the intima, media, and adventitia of the femoral artery at the radiated point were intact.

## 4 Discussion

We used P-32 as a radioactive source to irradiate normal myocardial tissue, and the immediate effects on cardiomyocytes were not obvious. At 30 days after the procedure, the voltage mapping results showed that P-32 internal radiotherapy can significantly reduce the local myocardial potential and produce different degrees of fibrosis in the irradiated myocardium. Specifically, 13 mCi of radiation for 60 min or 26 mCi of radiation for 30 min can result in complete transmural damage. However, 13 mCi of radiation for 30 min exhibited obvious damage only to the endocardium, not to the epicardium, which indicated that upregulation of the radiation dose of P-32 internal radiotherapy will increase the range of myocardial damage, even to the extent of transmural damage. Therefore, if P-32 internal radiotherapy is used to irradiate the origin of tachyarrhythmia or the key isthmus, it could also cause effective damage, thereby potentially playing a role in the treatment of tachyarrhythmia.

P-32 has been used as a radioactive source for skin keloids, rheumatoid arthritis, hemangioma, and myeloma. It is a relatively safe radioactive source with a short radiation distance and good controllability. Additionally, the half-life of P-32 is only 14.3 days. Therefore, compared with other radionuclides, there are fewer long-term adverse effects, and the post-processing of radionuclide waste is easier. During the experiments, the pigs did not experience any serious complications, thus indicating the good safety of P-32 internal radiotherapy.

We also found that P-32 internal radiotherapy had little effect on the coronary artery and femoral artery. Therefore, it may have an important role in the treatment of tachyarrhythmia originating from around the coronary artery and may be preferable compared to RFCA.

P-32 internal radiotherapy has several advantages. First, P-32 internal radiotherapy did not cause significant damage to the arteries. Immediately after the procedure, the gross specimen showed no fibrotic damage or acute or chronic thrombosis at the local coronary arteries in the irradiated area. It is suggested that the sensitivity of P-32 internal radiotherapy to the coronary artery is lower than that of myocardial tissue. The relative selectivity of different tissues also increases the advantages of P-32 internal radiotherapy compared with conventional RFCA. If the radiofrequency ablation sites are close to the coronary arteries, then RFCA may cause acute coronary artery damage, leading to acute myocardial infarction. P-32 internal radiotherapy may have an unparalleled advantage because the diameter of the radiotherapy catheter is 6 Fr. If it is extended into the coronary artery for irradiation, then it will cause acute myocardial infarction. Therefore, it is impossible to directly verify the coronary artery damage caused by P-32. The histopathological structures of the pig femoral artery and coronary artery are relatively similar, thereby making it more convenient and easier to explore the safety of P-32 in arteries. Therefore, to indirectly verify coronary artery damage caused by P-32 internal radiotherapy, we subjected the femoral arteries of pigs 4 to 7 to 26 mCi of radiation for 30 min. At 30 days later, femoral artery

angiography showed that the femoral artery did not exhibit stenosis or serious damage and had an intact vascular structure under microscopy. Furthermore, the safe use of coronary radioactive stents (with the same mechanism as P-32, which can emit  $\beta$ -rays) also proved that the damage caused by internal radiotherapy to the coronary artery is controllable. Ventricular tachycardia originates from some specific anatomic regions, such as the summit area, where the coronary artery distributes widely, or the epicardium, where adipose tissue is covered. RFCA can easily cause coronary injury that can result in acute myocardial infarction. With other methods, the radiofrequency energy can hardly penetrate the epicardium during routine endocardial ablation. Therefore, P-32 internal radiotherapy may have an important role in solving the shortcomings of RFCA. For example, internal radiotherapy can control the damage to the coronary artery. Additionally, unlike radiofrequency energy,  $\beta$ -rays can penetrate adipose tissue and affect arrhythmia originating from the epicardium of the left ventricle.

RFCA uses radiofrequency energy to damage the myocardium, thus causing local myocardial necrosis to treat ventricular arrhythmia. It requires a radiofrequency ablation catheter to be closely attached to the ventricular wall. If the attachment is not sufficient, then the radiofrequency energy cannot appropriately affect the myocardium, thereby causing damage. For tachyarrhythmia originating from some specific structures, such as the papillary muscles, the difficulty of routine RFCA is high and there are many requirements that must be fulfilled by the operator. In contrast to radiofrequency energy, P-32 internal radiotherapy can release  $\beta$ -rays to damage the cardiomyocyte DNA. Although poor adhesion reduces the effects of  $\beta$ -rays on the irradiation area per unit of time, compared with radiofrequency energy, there are fewer effects. Therefore, there are fewer requirements for P-32 internal radiotherapy catheter attachment than there are for radiofrequency ablation catheter attachment, which makes the catheter attachment procedure less difficult. This can be advantageous for patients who experienced failed RFCA because of insufficient catheter attachment.

Patients may feel better during internal radiotherapy. The immediate effects and tissue damage caused by P-32 internal radiotherapy are minimal. During the procedure, patients do not experience the adverse reactions caused by conventional radiofrequency ablation, such as nausea, vomiting, chest tightness, chest pain, and pericardial tamponade[16].

This study has some shortcomings. First, the number of experimental animals is relatively small, and the effects of different doses on cardiomyocytes have not been investigated in detail. Second, the time effect of tissue damage after internal radiotherapy is not fully understood. We plan to perform another study in which we will adjust the observation time gradient to find the exact time point at which the maximum effects of internal radiotherapy appear. Third, the distance and direction of irradiation are not presently controllable. Fourth, the radioactive catheter used during this study was independently designed and manufactured. It has a titanium tip surface, a length of 8 mm, and a diameter of 0.8 mm. The hardness of the tip may be greater than that of the radiofrequency ablation catheter, which may result in a hematoma on the endocardial surface of the myocardium at some of the irradiation points.

## 5 Conclusion

P-32 internal radiotherapy can cause transmural damage, change the electrical properties of cardiomyocytes, and has little effect on the coronary artery. Therefore, it is expected to be a complementary or alternative novel treatment for patients with tachyarrhythmia who have difficulty with routine radiofrequency ablation.

## Abbreviations

P-32: phosphorus-32

RFCA: radiofrequency catheter ablation

SBRT: stereotactic body radiotherapy

## Declarations

### Acknowledgments

The authors thank Dr. Xiaobo Jiang and Yejun Yan for their invaluable help during the experiment.

### Conflict of interest None

**Ethics Approval** All institutional guidelines for the care and use of laboratory animals were followed and approved by the ethical committee of West China Hospital, Sichuan university.

### Sources of Funding

This work was funded by the Study on Accurate Diagnosis and Treatment of Atrial Fibrillation (research subject number: JH2018040).

### Data availability statements

All data generated or analyzed during this study are included in this published article and/or its supplementary information files

## References

1. Guandalini G. S., Liang J. J., Marchlinski F. E.(2019). Ventricular tachycardia ablation: Past, present, and future perspectives. *JACC Clin Electrophysiol*, 5(12):1363-1383.  
<https://doi.org/10.1016/j.jacep.2019.09.015>
2. Gordon J. P., Liang J. J., Pathak R. K., Zado E. S., Garcia F. C., Hutchinson M. D., et al.(2018). Percutaneous cryoablation for papillary muscle ventricular arrhythmias after failed radiofrequency catheter ablation. *Journal of cardiovascular electrophysiology*, 29(12):1654-1663.  
<https://doi.org/10.1111/jce.13716>

3. Richter D., Lehmann H. I., Eichhorn A., Constantinescu A. M., Kaderka R., Prall M., et al.(2017). Ecg-based 4d-dose reconstruction of cardiac arrhythmia ablation with carbon ion beams: Application in a porcine model. *Phys Med Biol*, 62(17):6869-6883. <https://doi.org/10.1088/1361-6560/aa7b67>
4. Hohmann S., Deisher A. J., Suzuki A., Konishi H., Rettmann M. E., Merrell K. W., et al.(2019). Left ventricular function after noninvasive cardiac ablation using proton beam therapy in a porcine model. *Heart Rhythm*, 16(11):1710-1719. <https://doi.org/10.1016/j.hrthm.2019.04.030>
5. Borlich M., Sommer P.(2019). Cardiac mapping systems: Rhythmia, topera, ensite precision, and carto. *Card Electrophysiol Clin*, 11(3):449-458. <https://doi.org/10.1016/j.ccep.2019.05.006>
6. Sacher F., Gandjbakhch E., Maury P., Jenny C., Khalifa J., Boveda S., et al.(2021). Focus on stereotactic radiotherapy: A new way to treat severe ventricular arrhythmias? *Arch Cardiovasc Dis*, 114(2):140-149. <https://doi.org/10.1016/j.acvd.2020.11.003>
7. Krug D., Blanck O., Demming T., Dottermusch M., Koch K., Hirt M., et al.(2020). Stereotactic body radiotherapy for ventricular tachycardia (cardiac radiosurgery) : First-in-patient treatment in germany. *Strahlenther Onkol*, 196(1):23-30. <https://doi.org/10.1007/s00066-019-01530-w>
8. Blanck O., Buergy D., Vens M., Eiding L., Zaman A., Krug D., et al.(2020). Radiosurgery for ventricular tachycardia: Preclinical and clinical evidence and study design for a german multi-center multi-platform feasibility trial (raventa). *Clin Res Cardiol*, 109(11):1319-1332. <https://doi.org/10.1007/s00392-020-01650-9>
9. van der Ree M. H., Blanck O., Limpens J., Lee C. H., Balgobind B. V., Dieleman E. M. T., et al.(2020). Cardiac radioablation-a systematic review. *Heart Rhythm*, 17(8):1381-1392. <https://doi.org/10.1016/j.hrthm.2020.03.013>
10. Miszczyk M., Jadczyk T., Gołba K., Wojakowski W., Wita K., Bednarek J., et al.(2021). Clinical evidence behind stereotactic radiotherapy for the treatment of ventricular tachycardia (star)-a comprehensive review. *J Clin Med*, 10(6). <https://doi.org/10.3390/jcm10061238>
11. Lydiard P. S., Blanck O., Hugo G., O'Brien R., Keall P.(2021). A review of cardiac radioablation (cr) for arrhythmias: Procedures, technology, and future opportunities. *Int J Radiat Oncol Biol Phys*, 109(3):783-800. <https://doi.org/10.1016/j.ijrobp.2020.10.036>
12. Knutson N. C., Samson P. P., Hugo G. D., Goddu S. M., Reynoso F. J., Kavanaugh J. A., et al.(2019). Radiation therapy workflow and dosimetric analysis from a phase 1/2 trial of noninvasive cardiac radioablation for ventricular tachycardia. *Int J Radiat Oncol Biol Phys*, 104(5):1114-1123. <https://doi.org/10.1016/j.ijrobp.2019.04.005>
13. Chalkia M., Kouloulis V., Tousoulis D., Deftereos S., Tsiachris D., Vrachatis D., et al.(2021). Stereotactic arrhythmia radioablation as a novel treatment approach for cardiac arrhythmias: Facts and limitations. *Biomedicines*, 9(10). <https://doi.org/10.3390/biomedicines9101461>
14. Murray I., Du Y.(2021). Systemic radiotherapy of bone metastases with radionuclides. *Clin Oncol (R Coll Radiol)*, 33(2):98-105. <https://doi.org/10.1016/j.clon.2020.11.028>
15. Fassbender M. E.(2020). Guest edited collection: Radioisotopes and radiochemistry in health science. *Sci Rep*, 10(1):340. <https://doi.org/10.1038/s41598-019-56278-1>

## Figures

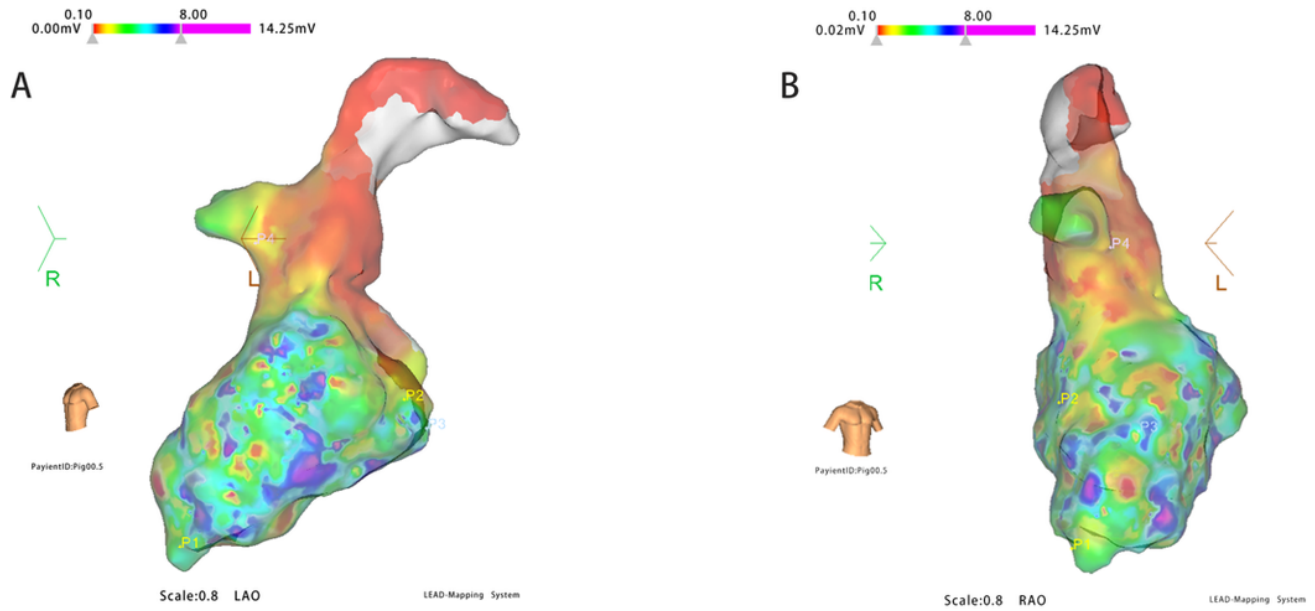


**Figure 1**

Voltage mapping of the left ventricle of experimental pig 1 before radiotherapy. (a) Left anterior oblique (LAO) position. (b) Right anterior oblique (RAO) position

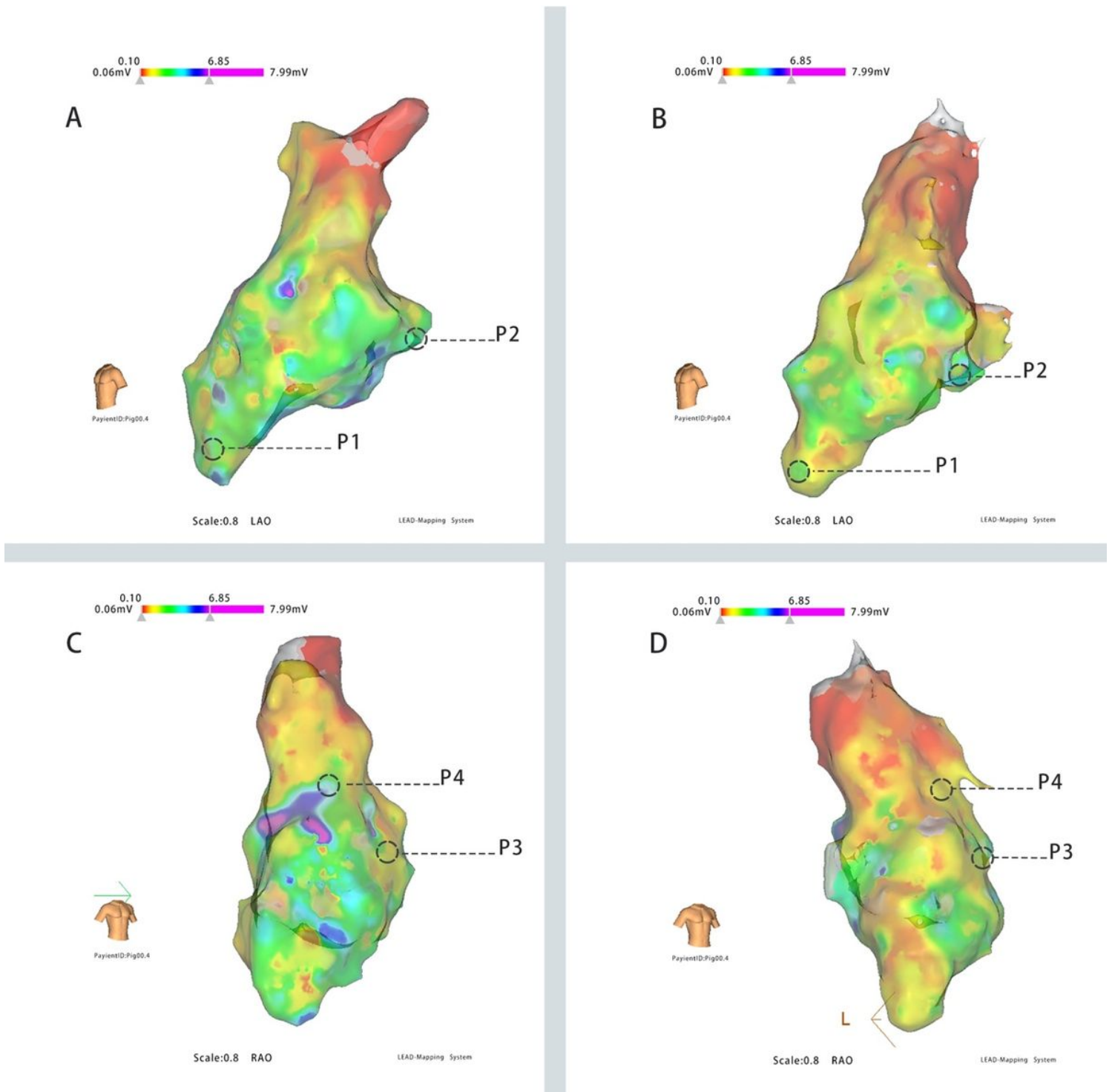


**Figure 2**

Mapping of the left ventricle in the left anterior oblique (LAO) and right oblique (RAO) positions of experimental pig 2 before and immediately after the procedure. (a and c) Voltage map before the procedure. (b and d) Voltage map after the procedure. The black circle indicates the two irradiated points (P1: the apex point; P2 and P3: two points around the mitral valve circus; p4: the point around the left coronary sinus). The voltage changes before and after irradiation are not significant

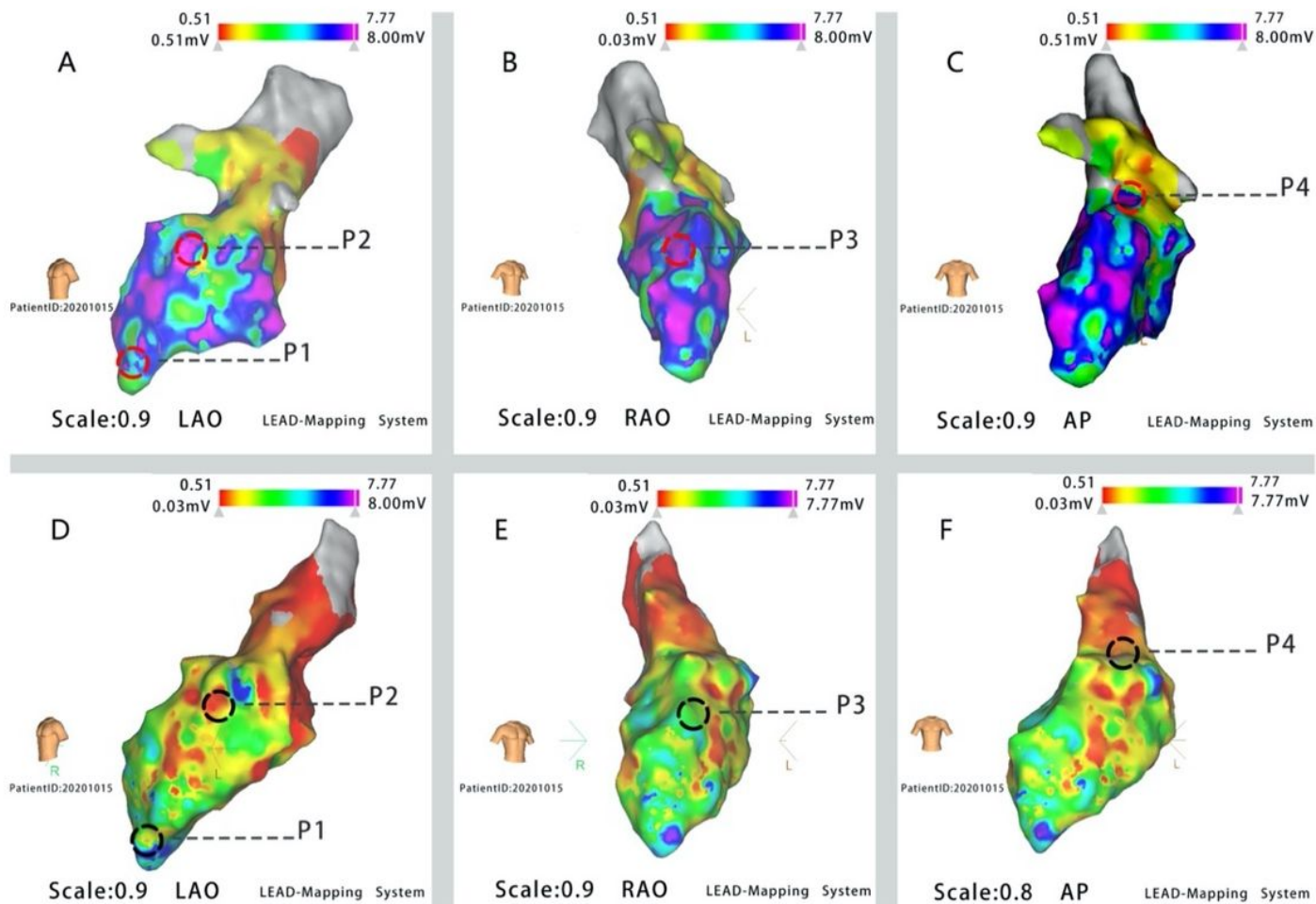


**Figure 3**

Voltage map of experimental pig 3 before and 30 days after the procedure. (a, b, and c). Voltage mapping before the procedure and (d, e, and f) 30 days after the procedure; P1, P2, P3, and P4 indicate four irradiated points of the left ventricle (P1: the apex point; P2 and P3: two points around the mitral valve circus; p4: point around the left coronary sinus). The voltage for all irradiated points at 30 days after the procedure was significantly lower than that before irradiation (Tables 5 and 6)

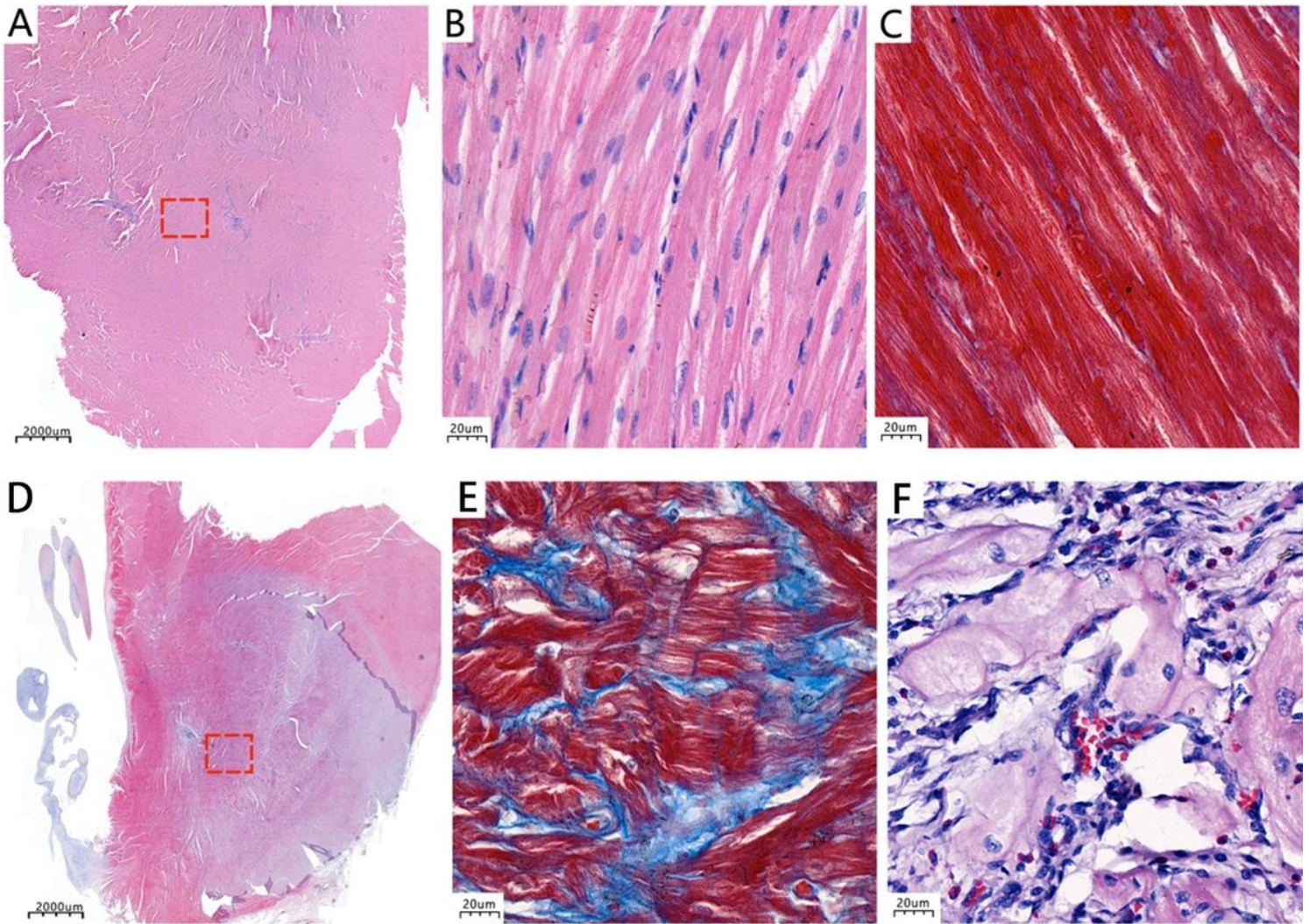


**Figure 4**

Pathological results of the mitral valve annulus irradiation site in pig 1 (a, b and c) and apex irradiation site in pig 5(d, e and f) at 30 days after the procedure. (a and b) Hematoxylin and eosin staining viewed using microscopy. Different degrees of inflammatory cell infiltration were observed using microscopy, including neutrophils, a few eosinophils, lymphocytes, and mononuclear macrophages. Parts of the myocardial tissue showed atrophy and muscle fiber breakage around the irradiated points. (c) Masson staining viewed under 400× magnification. The fibers of the valve tissue were stained blue, and the arrangement was slightly irregular. (d and f) Hematoxylin and eosin staining viewed under 4× and 400× magnification, respectively. (e) Masson staining viewed under 400× magnification. The myocardial fibers are obviously thinning and exhibit atrophy. The blue-stained fibrous tissue proliferates in a coarse grid and is arranged in a disorderly manner.

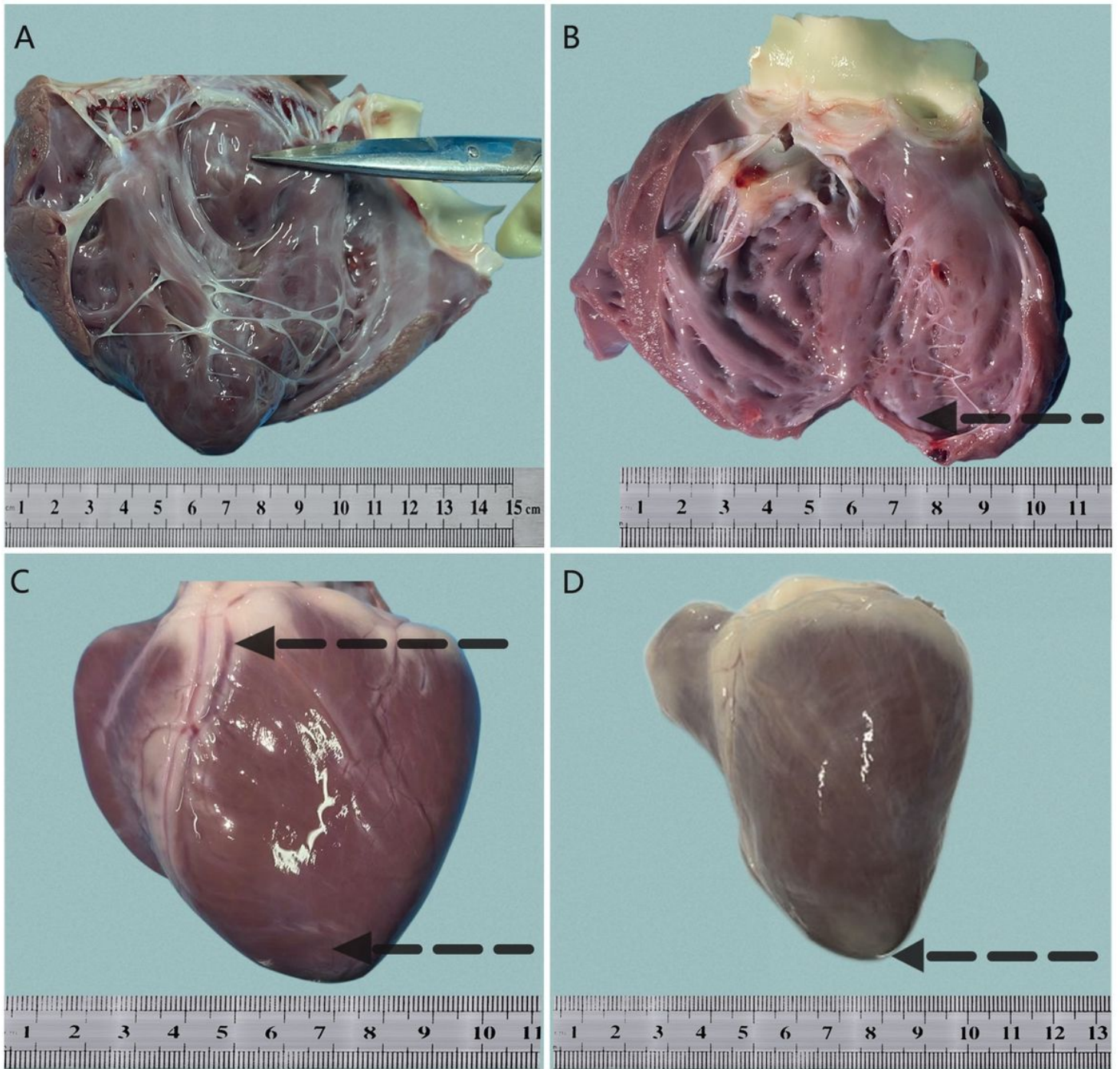


**Figure 5**

Gross specimen 30 days after the procedure. (a) Pathological changes at the mitral valve annulus on the intimal surface of pig 2. Obvious fibrotic changes of the intimal surface were clearly visible to the naked eye; no obvious pathological changes were seen on the epicardial surface. It is speculated that the radiation dose used for experimental pig 2 was small and failed to cause transmural damage. (c) Pathological changes of the epicardial surface of the apex of pig 4 (black arrow at the apex). Fibrosis was clearly visible to the naked eye. The upper black arrow indicates the left coronary artery that is structurally intact without obvious pathological changes. (b and d) Pathological changes of the inner and

outer membranes of the apex of experimental pig 5. A hematoma was observed on the endocardium surface at the irradiated sites, which might have resulted from long extrusion force between the tips of the radioactive catheter and the intimal surface of the myocardium

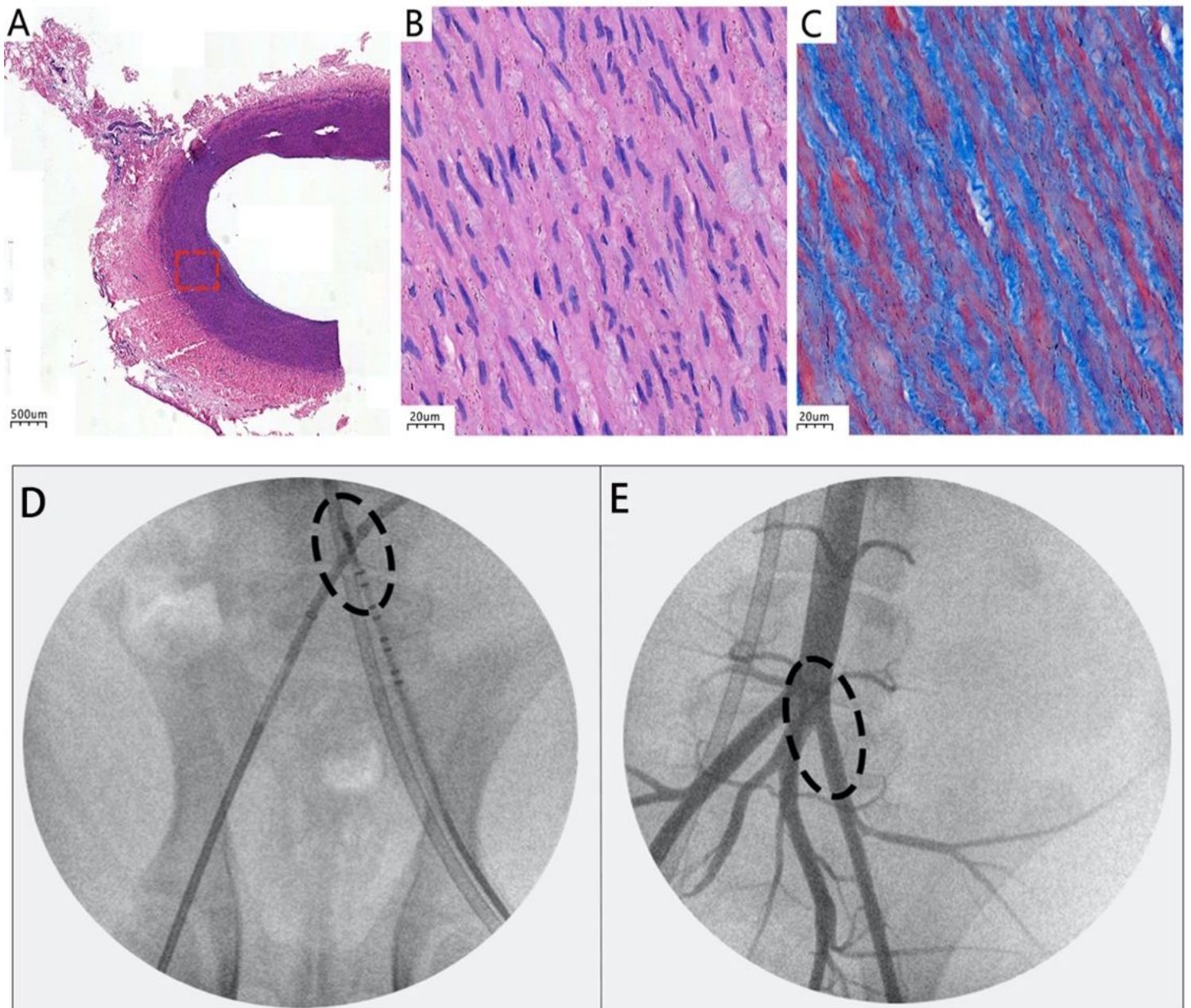


**Figure 6**

Effects of phosphorus-32 internal radiotherapy on the coronary artery (a, b and c) and femoral artery (d and f). The intima, media, and adventitia at the proximal left anterior descending artery are intact according to hematoxylin and eosin staining viewed under a microscope at 30 days after radiation (a and b). Masson staining revealed that cardiomyocytes at the intima were partly damaged and arranged in a disorderly manner when viewed under 400× magnification (c). Femoral arteriography after the procedure showing no significant stenosis before (d) or 30 days after radiation (f). The black circle indicates the irradiated sites of the femoral artery.